High-Speed Compressible Flow Solutions by Combined Characteristic-Based Split Method and Adaptive Meshing Technique

Parinya BOONMARLERT Sutthisak PHONGTHANAPANICH
Pramote DECHAUMPHAI*

Department of Mechanical Engineering, Faculty of Engineering,

Chulalongkorn University 10330, Thailand

Tel: 0-2218-6621 Fax: 0-2218-6621 E-mail: fmepdc@eng.chula.ac.th

Abstract

A finite element method for solving inviscid high-speed compressible flow problems is presented. The finite element equations corresponding to these flow problems were derived from the governing Euler equations that consist of the conservation of mass, momentums, and energy using the characteristic-based split method for the three-nodes triangular element. An adaptive meshing technique was combined with the finite element method to improve the solution accuracy and to reduce the computational time as well as the computer memory. The efficiency of the combined method is evaluated by the examples of an oblique shock reflection at a wall, a Mach 2.0 flow in a channel with compression and expansion ramps, and a shock-shock interaction on a cylinder.

1. Introduction

High-speed compressible flows normally include complex flow phenomena, such as shock waves, flow expansions, and shock-shock interactions [1]. Effects of these phenomena are critical in the design of high-speed vehicle structures. These flows are characterized by steep solution gradients that need robust analyses and computational techniques as well as dense meshes to obtain good resolution of flow behaviors. In the past decades, several finite element algorithms were developed to alleviate the computational effort due to complex flow filed, such as the Taylor-Galerkin [2], the Petrov-Galerkin [3], the least-squares [4], the cell-centered upwinding algorithms [5] and the characteristic-based split algorithm [6].

The characteristic-based split algorithm or the "CBS algorithm" is selected for solutions in this paper due to its capability to provide flow solution accuracy for most of the fluid dynamics problems. An adaptive meshing technique is combined with the CBS algorithm to improve the finite element solution accuracy and to reduce the computational time as well as the required computer memory. The adaptive meshing technique is applied to generate small elements in the regions of large change in the solution gradients to increase the solution accuracy, while larger elements are generated in the other regions. The paper starts by explaining the theoretical formulation for inviscid high-speed compressible flow analysis and the algorithm procedure. The basic idea behind the adaptive meshing technique is then described. Finally, the combined procedure is evaluated by analyzing the three examples of high-speed compressible flows; an oblique shock reflection at a wall, a Mach 2.0 flow in a channel with compression and expansion ramps, and a shock-shock interaction on a cylinder. The predicted solutions are compared with the exact solutions, and the experimental results.

2. Governing Differential Equations

The Euler equations for inviscid compressible flow are governed by the conservation of mass, momentums and energy. These equations, in two dimensions, are written in the conservation form as,

$$\frac{\partial}{\partial t}\{U\}+\frac{\partial}{\partial x}\{E\}+\frac{\partial}{\partial y}\{F\}=0 \qquad (1)$$

The vector $\{U\}$ contains the conservation variables defined by,

$$\{U\}^T = \lfloor \rho \quad \rho u \quad \rho v \quad \rho \varepsilon \rfloor \qquad (2)$$

where ρ is the fluid density, u and v are the velocity components in the x and y directions, respectively, and ε is the total energy of the fluid. The vectors $\{E\}$ and $\{F\}$ consist of

* Professor, Mechanical Engineering Department,
Chulalongkorn University Bangkok 10330

inviscid fluxes in the x and y directions, respectively. These inviscid flux vectors are given by,

$$\{E\}^T = \lfloor \rho u \quad \rho u^2 + p \quad \rho uv \quad \rho u\varepsilon + pu \rfloor \quad (3)$$

and

$$\{F\}^T = \lfloor \rho v \quad \rho uv \quad \rho v^2 + p \quad \rho v\varepsilon + pv \rfloor \quad (4)$$

where p is the pressure. The total energy consists of the internal energy and the kinetic energy defined by,

$$\varepsilon = e + \frac{1}{2}\left(u^2 + v^2\right) \quad (5)$$

The internal energy is assumed to satisfy the equation of state that can be written in the form,

$$e = \frac{p}{\rho(\gamma - 1)} \quad (6)$$

where γ is a specific heat ratio.

3. Computational Procedure

The basic concept of the CBS algorithm is to use the characteristic-Galerkin process to establish recurrence relations for temporal discretization, and the method of weighted residuals with Galerkin's criteria is used for spatial discretization for deriving the finite element equations.

3.1 The temporal discretization

The CBS algorithm for the compressible flow analysis consists of four steps. In the first step, the intermediate values of conservative variables of the momentum equations are calculated by omitting the pressure gradient terms. In the second step, the continuity equation is solved to determine the density changes in the fluid. In the third step, the conservative variables of the momentum equations are updated. Finally, the energy equation is solved for the total energy and the pressure is calculated by using the equation of state. These four steps in the fully explicit form can be written as follows [7],

Step 1: Solve the intermediate momentum equations,

$$\Delta U_i^* = \Delta t\left[-\frac{\partial\left(u_j U_i\right)}{\partial x_j} + \frac{\Delta t}{2}u_k \frac{\partial}{\partial x_k}\left(\frac{\partial\left(u_j U_i\right)}{\partial x_j} + \frac{\partial p}{\partial x_i}\right)\right]^n \quad (7)$$

where U_i are the mass fluxes.

Step 2: Solve the continuity equation,

$$\Delta\rho = \Delta t\left[-\frac{\partial U_i}{\partial x_i} - \theta\frac{\partial \Delta U_i^*}{\partial x_i} + \Delta t\,\theta\frac{\partial^2 p}{\partial x_i \partial x_i}\right]^n \quad (8)$$

where θ is between 0.5 and 1.

Step 3: Solve the momentum correction equations,

$$\Delta U_i = \Delta U_i^* - \Delta t\left[\frac{\partial p_i}{\partial x_i}\right]^n \quad (9)$$

Step 4: Solve the energy equation,

$$\Delta\rho\varepsilon = \Delta t\left[-\frac{\partial\left(\rho u_i \varepsilon\right)}{\partial x_i} - \frac{\partial\left(u_i p\right)}{\partial x_i} + \frac{\Delta t}{2}u_k \frac{\partial}{\partial x_k}\left(\frac{\partial\left(\rho u_i \varepsilon\right)}{\partial x_i} + \frac{\partial\left(u_i p\right)}{\partial x_i}\right)\right]^n \quad (10)$$

3.2 The spatial discretization

The three-nodes triangular element is used in this study. The element assumes linear interpolation for the variable U, E, F and p as,

$$U = N_\alpha(x,y)\,U_\alpha \quad (11a)$$
$$E = N_\alpha(x,y)\,E_\alpha \quad (11b)$$
$$F = N_\alpha(x,y)\,F_\alpha \quad (11c)$$
$$p = N_\alpha(x,y)\,p_\alpha \quad (11d)$$

where $\alpha = 1,2,3$ and N_α is the element interpolation functions.

The method of weighted residuals with Galerkin's criteria is employed to discretize the finite element equations by multiplying Eqs. (7)-(10) with the weighting function, N_α, and performing integration by parts using the Gauss theorem to yield the element equations in the steps below,

Step 1: Solve the intermediate momentum equations,

$$[M]\{\Delta U_i^*\} = \Delta t\left[\left([C]-[S]\right)\{u_j U_i\} - \frac{\Delta t}{2}u_k\left[[K_u]\{u_j U_i\} - [T_u]\{u_j U_i\} + \left([K_p]-[T_p]\right)\{p\}\right]\right]^n \quad (12)$$

Step 2: Solve the continuity equation,

$$[M]\{\Delta\rho\} = \Delta t\left[\left([D]-[R_u]\right)\{U_i + \theta\Delta U_i^*\} - \Delta t\,\theta[K]\{p\}\right]^n \quad (13)$$

Step 3: Solve the momentum correction equations,

$$[M]\{U_i\} = [M]\{\Delta U_i^*\} + \Delta t\left[([D]-[R_u])\{p\} \right]^n \quad (14)$$

Step 4: Solve the energy equation,

$$[M]\{\Delta\rho\varepsilon\} = \Delta t\Big[([C]-[S])\{u_j(\rho\varepsilon+p)\} - \frac{\Delta t}{2}u_k([K_u]-[T_u])\{u_j(\rho\varepsilon+p)\} \Big]^n \quad (15)$$

In above equations, the element matrices can be written in the integral form as,

$$[M] = \int_\Omega \{N\}\lfloor N\rfloor d\Omega \quad (16a)$$

$$[C] = \int_\Omega \left\{\frac{\partial N}{\partial x_j}\right\}\lfloor N\rfloor d\Omega \quad (16b)$$

$$[D] = \int_\Omega \left\{\frac{\partial N}{\partial x_i}\right\}\lfloor N\rfloor d\Omega \quad (16c)$$

$$[K] = \int_\Omega \left\{\frac{\partial N}{\partial x_i}\right\}\left\lfloor \frac{\partial N}{\partial x_i}\right\rfloor d\Omega \quad (16d)$$

$$[K_u] = \int_\Omega \left\{\frac{\partial N}{\partial x_k}\right\}\left\lfloor \frac{\partial N}{\partial x_j}\right\rfloor d\Omega \quad (16e)$$

$$[K_p] = \int_\Omega \left\{\frac{\partial N}{\partial x_k}\right\}\left\lfloor \frac{\partial N}{\partial x_i}\right\rfloor d\Omega \quad (16f)$$

$$[S] = \int_\Gamma \{N\}\lfloor N\rfloor n_j\, d\Gamma \quad (16g)$$

$$[R_u] = \int_\Gamma \{N\}\lfloor N\rfloor n_i\, d\Gamma \quad (16h)$$

$$[T_u] = \int_\Gamma \{N\}\left\lfloor \frac{\partial N}{\partial x_j}\right\rfloor n_k\, d\Gamma \quad (16i)$$

$$[T_p] = \int_\Gamma \{N\}\left\lfloor \frac{\partial N}{\partial x_i}\right\rfloor n_k\, d\Gamma \quad (16j)$$

An artificial diffusion is also needed in the algorithm to reduce oscillation of the solutions especially near the shock wave. The second derivative of pressure [8] is selected to contribute the artificial diffusion into nodal quantities. These nodal artificial diffusions are determined from,

$$[M]\left\{\frac{U_s^{n+1}-U^{n+1}}{\Delta t}\right\} = C_e h^3 \frac{|V|+c}{\bar{p}}\left|\nabla^2 p\right|_e [K]\{U\}^n \quad (17)$$

where U_s^{n+1} is the modified solution at time step $n+1$ after adding artificial diffusion, U^{n+1} is the solution at time step $n+1$, C_e is the user-specified coefficient normally varies between 0.0 and 2.0, h is the element size, $|V|$ is the absolute velocity, c is the speed of sound, $\bar{p}$ is the average pressure, $\left|\nabla^2 p\right|_e$ is the second derivative of pressure over an element.

The fully explicit form of CBS algorithm is conditionally stable. The permissible time step is governed by,

$$\Delta t = \sigma\frac{h}{|V|+c} \quad (18)$$

where σ is the Courant number ($0<\sigma\leq 1$).

4. Adaptive Meshing Technique

For high-speed compressible flows, the flow properties, such as the density changes abruptly across the shock waves. Small elements are thus needed along to shock waves to capture accurate shock wave resolution. As small elements must be placed in the region where changes in the density gradients are large, thus the second derivatives of density at a point with respect to global coordinates x and y are needed. Using the concept of principal stresses determination from a given state of stresses at a point, the principal quantities in the principal directions X and Y where the cross-derivatives vanish are determined. The maximum principal quantities are then used to compute the proper element size h_i by requiring that the error should be uniform for all elements,

$$\begin{bmatrix} \frac{\partial^2\rho}{\partial x^2} & \frac{\partial^2\rho}{\partial x\partial y} \\ \frac{\partial^2\rho}{\partial x\partial y} & \frac{\partial^2\rho}{\partial y^2} \end{bmatrix} \Rightarrow \begin{bmatrix} \frac{\partial^2\rho}{\partial X^2} & 0 \\ 0 & \frac{\partial^2\rho}{\partial Y^2} \end{bmatrix} \quad (19)$$

This value is used to compute proper element size from the condition,

$$h_i^2\lambda_i = h_{min}^2\lambda_{max} = constant \quad (20)$$

In the above Eq. (20), λ_{max} is the maximum principal quantity for all elements and h_{min} is the minimum element size specified by users.

5. Results

To demonstrate the capability of the combined adaptive meshing technique and the characteristic-based split method for increasing the flow solution accuracy, three simulations of the steady-state high-speed compressible flows are used. (1) an oblique shock reflection at a wall, (2) a Mach 2.0 flow in a channel with compression and expansion ramps, and (3) a shock-shock interaction on a cylinder.

5.1 Oblique shock reflection at a wall

The problem statement of an oblique reflection at a wall is described in Fig. 1. The Mach 2.9 and 2.387 flows enter through the left and the top boundaries of computational domain resulting in an oblique shock from the top-left corner. This shock incidents and reflects at a wall as highlighted in the figure. The procedure starts by creating a relatively uniform mesh as shown in Fig. 2(a) that consists of 4,920 elements. The fluid analysis is then performed to generate the corresponding solution such as the density contours as shown in Fig. 2(b). The figure shows the computed shock is not sharp because the elements along the shock lines are not small enough. This flow solution is then used to generate an adaptive mesh to cluster small elements in the regions of sharp changes of the density gradients, and at the same time, to use larger elements on the other regions. The fluid analysis is then performed again to yield a more accurate solution. The entire process is repeated to generate the third adaptive mesh consisting of 19,882 elements and the corresponding solution as shown in Figs. 3(a)-(b), respectively. Figures 4a)-(b) show the predicted density and pressure distributions at y = 0.25 as compared to with the exact solutions.

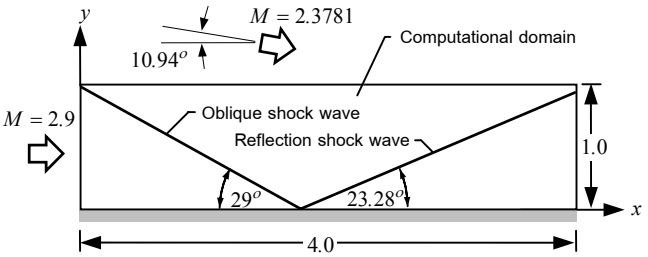

Fig. 1 Problem statement of an oblique shock reflection at a wall.

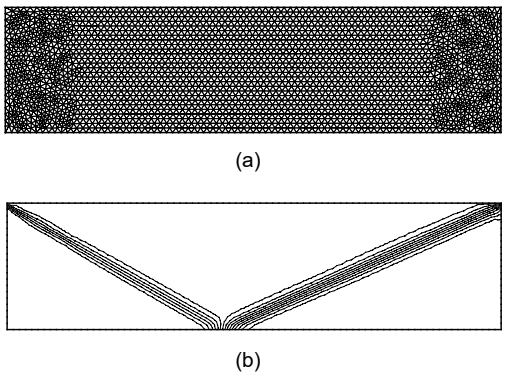

(a) (b)

Fig. 2 An oblique shock reflection at a wall: (a)-(b) Initial mesh and the corresponding density contours.

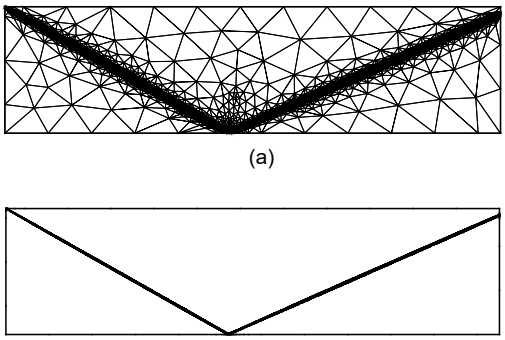

(a) (b)

Fig. 3 An oblique shock reflection at a wall: (a)-(b) Third adaptive mesh and the corresponding density contours.

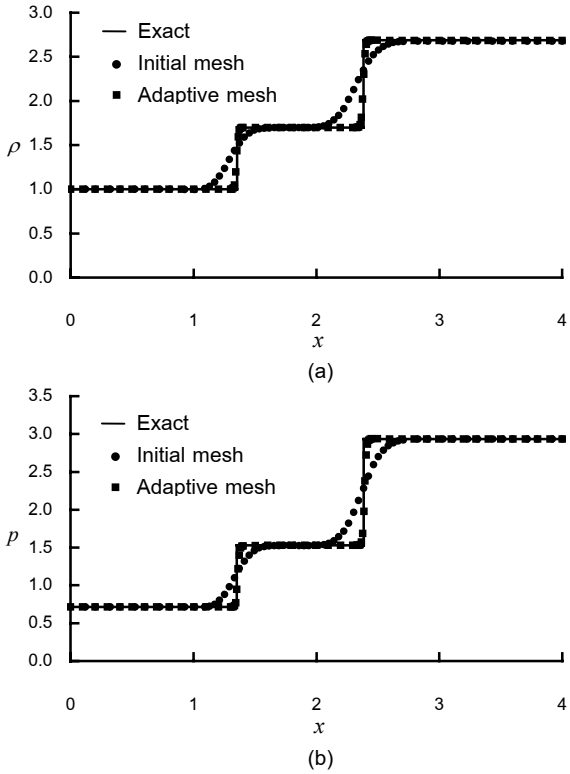

Fig. 4 Comparative solutions at y = 0.25 for an oblique shock reflection at a wall: (a) density distribution; (b) pressure distribution.

5.2 Mach 2.0 flow in a channel with compression and expansion ramps

The problem statement of a Mach 2.0 in a channel with compression and expansion ramps and the sketch of flow behavior are described in Fig. 5. The flow creates an oblique shock from the compression ramp that impinges at the upper wall resulting in a reflecting shock. The reflecting shock also intersects with the Mach waves generated from the expansion corner. The combined characteristic-based split method and

adaptive meshing technique starts from generating a relatively uniform mesh such as that shown in Fig. 6(a) with 5,578 elements. Fig. 6(b) shows the density contours of the corresponding flow solution obtained from the finite element mesh in Fig. 6(a). The figure shows that the computed shock waves are not sharp and mach waves resolution around expansion corner is not good due to the element sizes in these regions are too large. With such the solution, a new adaptive mesh was then constructed and the flow analysis was performed again. The same process was repeated for three times. The third adaptive finite element model consisting of 26,628 elements and the corresponding density contours are shown in Fig. 7(a)-(b), respectively.

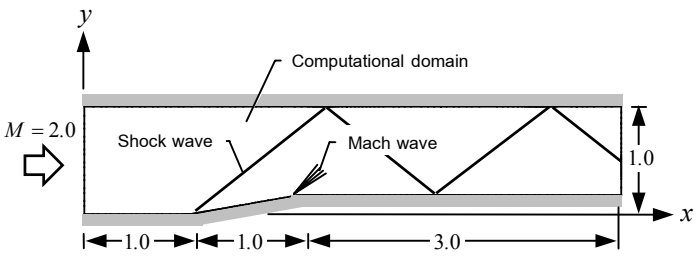

Fig. 5 Problem statement of a Mach 2.0 in a channel with compression and expansion ramps

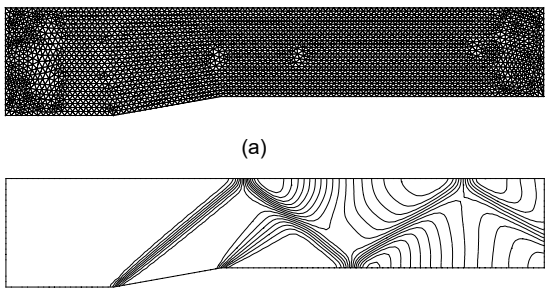

(a)

(b)

Fig. 6 Mach 2.0 in a channel with compression and expansion ramps: (a)-(b) Initial mesh and the corresponding density contours.

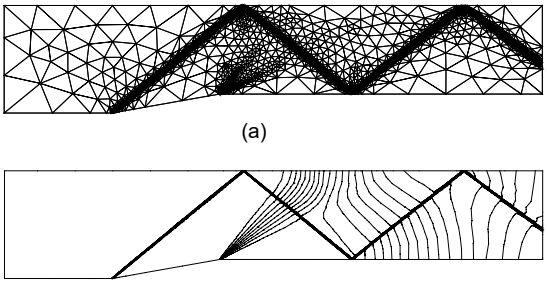

(a)

(b)

Fig. 7 Mach 2.0 in a channel with compression and expansion ramps: (a)-(b) Third adaptive mesh and the corresponding density contours.

5.3 Shock-shock interaction on a cylinder

The problem highlights the shock-shock interaction on a cylinder. The mainstream Mach number is 8.03 and the disturbed stream Mach number is 5.25 at angle of 12.5°. The problem statement of the flow is shown in Fig. 8. This represents a situation in which an oblique shock interacts with bow shock in front of the cylinder. The adaptive finite element model consisting of 40,359 elements is shown in Fig. 9(a). The corresponding pressure and Mach contours are presented in Figs. 9(b) and (c), respectively. Figure. 10 shows the predicted pressure on the surface of the cylinder comparing to the experimental data [9]. The predicted and experimental pressures are normalized by the undisturbed flow (no shock interaction) stagnation pressure. The figure shows good agreement of the pressure distributions and excellent agreement of the peak pressure locations.

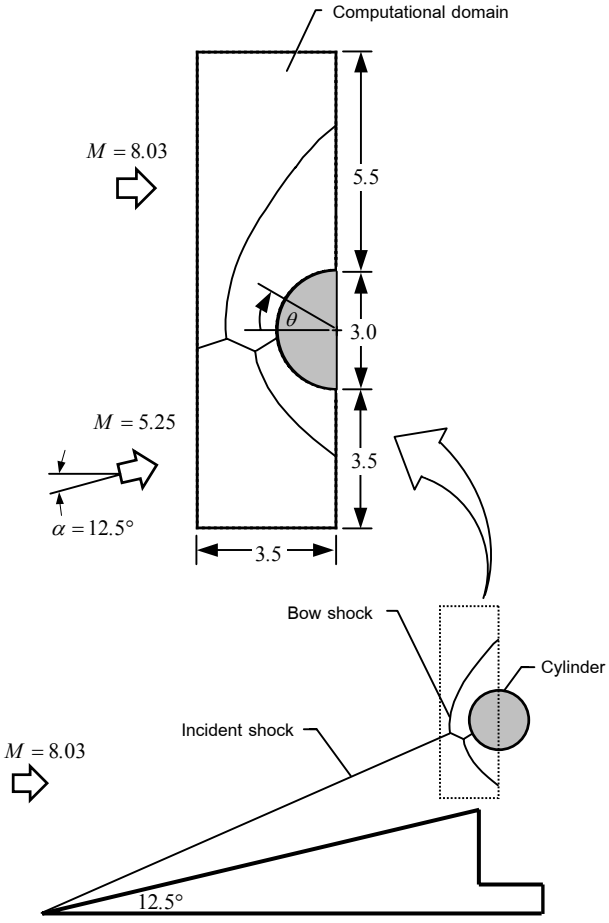

Fig. 8 Problem statement of a shock-shock interaction on a cylinder

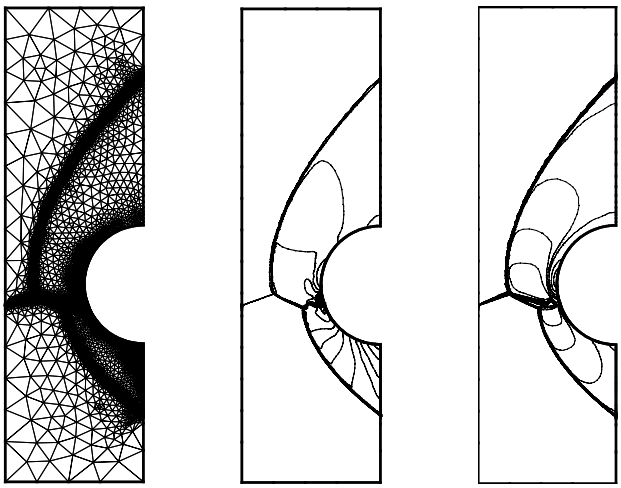

(a) (b) (c)

Fig. 9 Shock-shock interaction on a cylinder: (a) adaptive mesh (b)-(c) the corresponding pressure and Mach contours.

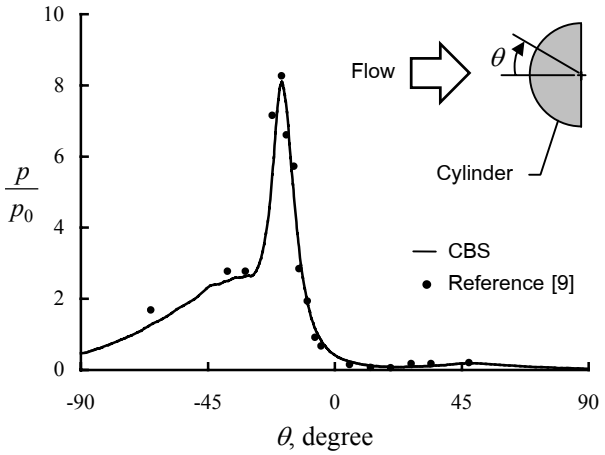

Fig. 10 Comparative pressure distributions along cylinder surface.

6. Conclusion

The finite element method based on the characteristic-based split algorithm for analysis of two-dimensional inviscid high-speed compressible flow was presented. The method was combined with an adaptive meshing technique to improve the flow solution accuracy and to reduce the computational time. The technique generates an entirely new mesh based on the solution obtained from a previous mesh. The new mesh consists of clustered elements in the regions with large change in the solution gradients to provide high solution accuracy. At the same time, larger elements are generated in the other regions to reduce the computational time. Three examples of high-speed compressible flows were presented to assess the effectiveness of the combined method. These examples are an oblique shock reflection at a wall, a Mach 2.0 flow in a channel with compression and expansion ramps, and a shock-shock interaction on a cylinder. These three examples demonstrate the combined method can provide high solution accuracy with reduced computational time and memory for analysis of high-speed compressible flow problems.

7. Acknowledgments

The authors are pleased to acknowledge the Thailand Research Fund (TRF) for supporting this research work.

8. References

[1] Anderson, J.D. Jr. Modern Compressible Flow with Historical Prospective. (2nd ed). New York: McGraw Hill.

[2] Donea, J. “A Taylor-Galerkin Method for Convective Transport Problems”, International Journal for Numerical Methods in Engineering, 1984, Vol. 20, pp. 101-119.

[3] Huges, T.J.R. “Recent Progress in the Development and Understanding of SUPG Methods with Special Reference to the Compressible Euler and Navier-Stokes Equations”, International Journal for Numerical Methods in Fluids, 1987, Vol. 7, pp. 1261-1275.

[4] Jiang, B.N. and Carey, G.F. “A Stable Last-Squares Finite Element Method for Non-Linear Hyperbolic Problems”, International Journal for Numerical Methods in Fluids, 1988, Vol. 8, pp. 933-942.

[5] Gnoffo, P.A. “Application of Program LUARA to Three-Dimensional AOTV Flow Fields”, AIAA Paper 86-0565, 1986.

[6] Zienkiewicz, O. C., Nithiarasu, P., Codina, R., Vazquez, M. and Ortiz, P. “The Characteristic-Based-Split Procedure: An Efficient and Accurate Algorithm for Fluid Problems”, International Journal for Numerical Methods in Fluids, 1999, Vol. 31, pp. 359-392.

[7] Satya Sai, B.V.K., Zienkiewicz, O. C., Manzari, M.T., Lyra, P.R.M. and Morgan, K. “General Purpose Versus Special Algorithms for High-Speed Flows with Shocks”, International Journal for Numerical Methods in Fluids, 1998, Vol. 27, pp. 57-80.

[8] Nithiarasu, P., Zienkiewicz, O.C., Satya Sai, B.V.K., Morgan, K., Codina, R.and Vazquez, M. “Shock Capturing Viscosities for the General Fluid Mechanics Algorithm”, International Journal for Numerical Methods in Fluids, 1998, Vol. 28, pp. 1325-1353.

[9] Dechaumphai, P. and Wieting, A. R. “Couple Fluid-Thermal-Structural Analysis for Aerodynamically Heated Structures”, 7th International Conference on Finite Element Methods in Flow Problems, Alabama, April 3-7, 1989.